

Qubit Mapping Toward Quantum Advantage

Chin-Yi Cheng¹, Chien-Yi Yang⁶, Ren-Chu Wang⁷, Yi-Hsiang Kuo¹,
Hao-Chung Cheng¹⁻⁵, and Chung-Yang (Ric) Huang¹

¹Department of Electrical Engineering, National Taiwan University, Taiwan

²Graduate Institute of Communication Engineering, National Taiwan University, Taiwan

³Center for Quantum Science and Engineering, National Taiwan University, Taiwan

⁴Physics Division, National Center for Theoretical Sciences, Taiwan

⁵Hon Hai (Foxconn) Quantum Computing Center, Taiwan

⁶Department of Computer Science and Engineering, University of California San Diego

⁷College of Computing, The Georgia Institute of Technology, USA

james31423a@gmail.com, chy036@ucsd.edu, renruewang@gatech.edu, b08901173@ntu.edu.tw,

haochung.ch@gmail.com, cyhuang@ntu.edu.tw

Abstract—Qubit Mapping is an essential step in realizing quantum circuits on actual hardware devices. However, due to the high complexity of this problem, current solutions can only work on circuits in fairly small scales (i.e. < 50 qubits). In this paper, we propose a qubit mapping methodology which, to the best of our knowledge, is the first framework to handle very large quantum circuits (i.e. thousands of qubits) towards the quantum advantage. Our novel routing algorithm, Duostra, can efficiently identify the optimal routing path for a given two-qubit gate to operate on physical qubits through swap-gate insertions, and our scheduling heuristic offers the flexibility to strike the balance in optimizing the performance and pursuing the scalability. Experimental results show that our method runs 10 times faster than the state-of-the-art approaches, while on average can still outperform them by over 5% in terms of the execution time of the quantum circuits. More specifically, our proposed algorithm can complete the qubit mapping of an 11,969-qubit Quantum Fourier Transform circuit within five hours.

Index Terms—Quantum Compilation, Qubit Mapping, Quantum Advantage, Scalability, Flexibility, Optimal Solution

I. INTRODUCTION

Quantum advantage is the holy grail of quantum computing. It refers to the ultimate goal where the quantum computers can solve a real-world problem exponentially faster than the classical ones [1] (e.g. Quantum Computing [2], Quantum Communication [3], Quantum Cryptography [4], and Quantum Machine Learning [5]). Recent advances on the capacity of quantum computing devices seem to ignite a spark of hope on the coming true of this dream – For example, IBM Osprey has reached the 433-qubit milestone [6], tripling its previous generation, Eagle, from last year. This is about $1/5$ of the 2048 qubits for the Quantum Fourier Transform (QFT) to break the RSA-1024 encryption [7] [8], and about 30% of the 255×6 qubits for the discrete logarithms over elliptic curves (e.g. Curve25519) to solve the Bitcoin encryption [9]. It looks like we are just a couple of years away from the quantum advantage.

However, in reality, the connectivity constraints on most of the quantum computing hardware nowadays have burst the bubble of the abovementioned expectation. For example, Fig. 1 is the retrieved topology of the *ibmq_washington* quantum

computer. Each vertex represents a physical qubit and is connected to at most three adjacent qubits. If the operation of a quantum gate in a quantum circuit is on two non-adjacent qubits, say qubits #0 and #126 in the extreme, we will need to perform a long sequence of swap operations to bring the computation to a pair of adjacent qubits, say qubits #61 and #62. This will result in a much higher demand on the number of qubits [10], and what is worse, lead to a much longer execution time of the quantum circuit. Therefore, how to intelligently map the quantum circuit to the physical qubits, called “qubit mapping problem”, will be the key to the success of the quantum advantage.

The qubit mapping is shown to be an NP-Complete problem [11], let alone the optimality on the number of required qubits and the execution time of the quantum circuit. Many researchers have been working toward the practicality of the qubit mapping algorithms. Li *et al.* [12] proposed SABRE¹ by heuristic of shortest path cost and look-ahead technique. This work becomes the general baseline for minimizing the circuit depth of a quantum circuit. However, in reality, it is not precise enough to represent the execution time of a quantum program by the circuit depth. Deng *et al.* [13] proposed CODAR² specifically for the total circuit execution time. They first introduced the concept of lock time for the busy qubits and defined different timing costs on common gates (i.e. 1, 2 and, 6 units for single-qubit, double-qubit, and swap gates, respectively). On the other hand, Zhang *et al.* further proposed the Time-Optimal Qubit Mapping (TOQM) [14] heuristic algorithm with estimated cost to achieve better results for circuit execution time. Although the above-mentioned algorithms claimed to achieve optimal mapping solutions, the runtime of their algorithms was very long due to the fact that they needed to calculate the costs of all the potential swapping candidates in each iteration of selecting a swap. As a consequence, they could only handle mapping problems up to 50 qubits, which was much smaller than the number of

¹SWAP-based **Bi**diREctional heuristic search algorithm

²COntext-sensitive and **D**uration-Aware **R**emapping algorithm

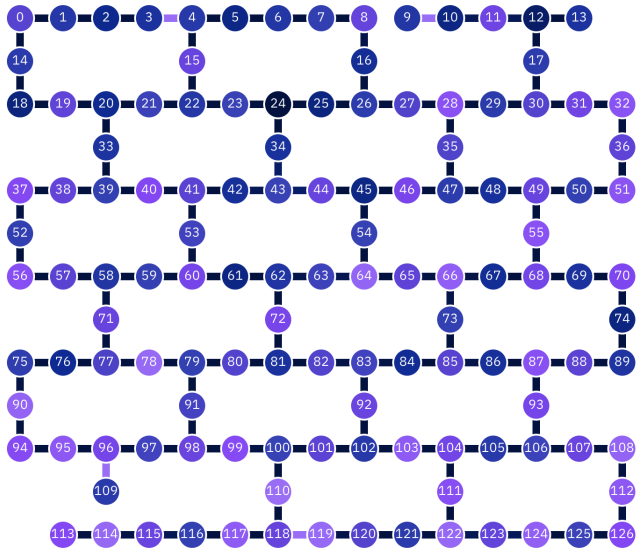


Fig. 1: The topology of *ibmq_washington*, retrieved from [15]

required qubits for achieving quantum advantage.

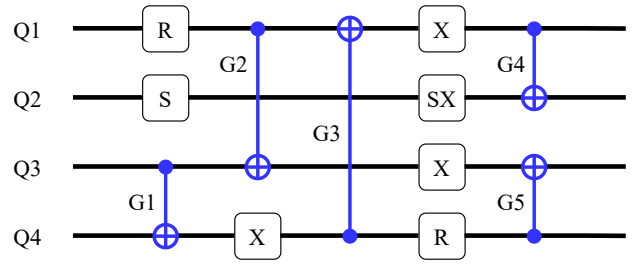
In this paper, we propose a powerful qubit mapping framework for better scalability and flexibility. Instead of optimizing by computing one swapping insertion one at a time like previous works, our novel routing algorithm, Duostra, directly computes the optimal route of a two-qubit gate and thus optimizes its swapping path at once. Furthermore, we incorporate a scheduler to determine the best execution sequence of the gates in order to optimize the total execution time on the quantum computing device. With scheduling heuristics to strike the balance between the optimality of the circuit execution time and the runtime of our algorithm, we are able to provide flexibility in handling various sizes of quantum circuits.

The experimental results show that our framework can outperform the IBM Qiskit Mapping on a 127-qubit QFT by 33%, and scales up to the problem size of 11,969 qubits within 5 hours (with time complexity $O(n^{2.8})$, where n represents the problem size). For the benchmark proposed by SABRE [12], our scheduler not only achieves an average 5% cost improvement compared to the state-of-the-art TOQM [14], but also finishes in only $1/8$ of the TOQM runtime. In conclusion, our proposed qubit mapping framework provides a solution towards quantum advantage by efficiently implementing ideal quantum algorithms on a non-fully connected quantum device.

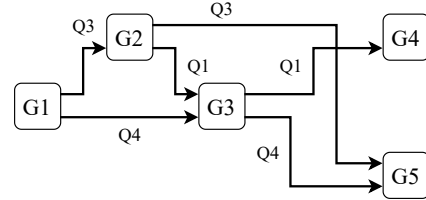
The rest of the paper is organized as follows. We first explain the qubit mapping problem in Section II. The proposed framework is detailed in Section III, and specifically the proof for the optimality of the Duostra algorithm is provided in Section IV. We present the experiment results in Section V, including scalability, performance, and flexibility, and we conclude the paper in Section VI.

II. QUBIT MAPPING PROBLEM

Given a quantum circuit composed from the gates of a quantum cell library (e.g. *Clifford+T* library), and a topology



(a) An example of a logical circuit



(b) Its corresponding Dependency Graph

Fig. 2: An example of the Dependency Graph.

of the qubits on a quantum computer (e.g. Fig. 1), the qubit mapping problem is to schedule the operations of the quantum gates and then assign them to the qubits on the quantum computer. However, since the computation of a two-qubit gate³ can only be performed on adjacent qubits of the actual hardware device (called “coupling constraint”), and yet the topology of the physical device often constrains its qubits to interact with only a small number of adjacent neighbors (e.g. 1 to 3 for *ibmq_washington* quantum computer as shown in Fig. 1) to 3 for *ibmq_washington* quantum computer as shown in Fig. 1), it is often that we need to insert additional SWAP gates to bring the logically-connected-but-physically-apart inputs of a two-qubit gate to the adjacent qubits.

For example, let’s assume $Q1$, $Q2$, $Q3$ and $Q4$ of the logical circuit in Fig. 2(a) are mapped to qubits #1, #2, #3 and #4 in Fig. 1, respectively. Since the inputs of $G2$ (i.e. a controlled-NOT (CX) gate) are not on adjacent qubits, we need to insert a SWAP gate either between qubits #1 and #2, or between #2 and #3 to resolve the coupling constraint. Clearly, we will have to insert SWAP gates for the following $G3$, and maybe for $G4$ and $G5$. We can also see that by choosing different SWAP insertions for $G2$ (i.e. between #1 and #2, or between #2 and #3), it will result in different numbers of SWAPs required for $G3$, $G4$ and $G5$. Minimizing the number of SWAP insertions is the core of the qubit mapping problem.

A SWAP is composed of three consecutive CX gates, where the middle CX possesses opposite control and target qubits with respect to the other two CX gates. The insertion of the SWAP gates greatly increases the gate counts and execution time of the quantum circuit. Therefore, the objective of the qubit mapping problem is to optimize the scheduling and

³Without loss of generality, we assume there are only single- and two-qubit gates in the quantum cell library.

mapping of the logical cells to the physical qubits and thus minimize the gate counts, execution time, and the resulting computing errors.

To illustrate our qubit mapping framework in the next section, we first introduce three data structures to facilitate the design of the qubit mapping algorithm:

1) *Dependency Graph (DepG)*: A graph that describes the computational dependency of the two-qubit gates in the quantum circuit. For the qubit mapping problem, since the single-qubit gates will never violate the coupling constraints, we only need to consider the two-qubit gates for SWAP insertions to bring their input qubits to the adjacencies. Take Fig. 2(a) as an example, the gate G_5 operates on two qubits, Q_3 and Q_4 . It can only be executed after all the previous gates (i.e. G_2 and G_3) are executed. We say G_5 depends on G_2 and G_3 , and add edges from G_2 and G_3 to G_5 to build a directed acyclic graph (DAG), called Dependency Graph as shown in Fig. 2(b). In a Dependency Graph, an edge $Gate_i \rightarrow Gate_j$ means that $Gate_j$ depends on $Gate_i$. A gate can be executed only after all its parents are executed.

2) *Device Graph (DevG)*: An undirected graph $DevG = (V, E)$ represents the topology of a real quantum computing device, where V denotes the physical qubits and E is the set of edges corresponding to the connectivity among physical qubits. A pair of qubits can be involved in the two-qubit operation only if there is a direct connection between these two qubits. In the qubit mapping problem, if a two-qubit operation is mapped to two non-adjacent physical qubits, we need to find a path between these two qubits on DevG to perform SWAPs.

3) *Waitlist (WL)*: Inspired by the “front layer” concept from [12], Waitlist is a list of gates that are ready for execution. That is, gates in a Waitlist are those without any unexecuted parents in the Dependency Graph. For example, if G_1 and G_2 were executed in Fig. 2, then G_3 is the only gate in the Waitlist. Since gates should be executed following the Dependency Graph, gates in the Waitlist are the only candidates when scheduling for the next execution.

III. THE PROPOSED QUBIT MAPPING FRAMEWORK AND ALGORITHM

Our proposed qubit mapping framework is shown in Fig. 3. Unlike previous studies which treat the qubit mapping problem as a whole, we propose a framework that decomposes the problem into more manageable subproblems – placement, routing, and scheduling. We start by quickly placing the circuit inputs to certain physical qubits, and from there we have the first set of gates in the Waitlist. While the Router can efficiently suggest a routing path that minimizes the execution time of a two-qubit gate on a real device, the Scheduler now only needs to consider the order of the gates for execution in the Waitlist. This framework offers great flexibility in choosing different scheduling and routing heuristics with different metrics for different quantum circuits. Below we present our design of algorithms for initial placement, scheduling, and routing.

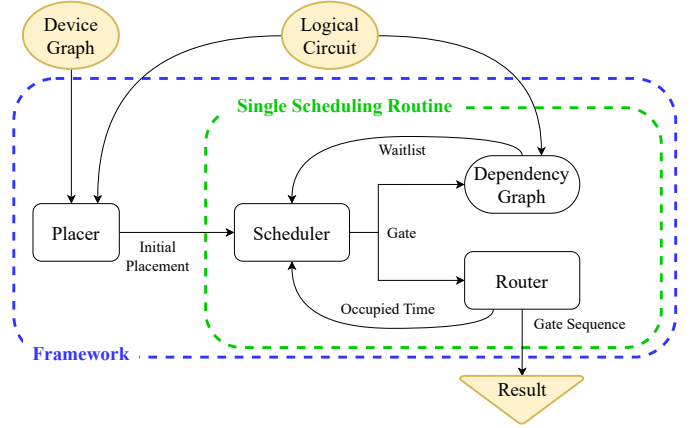


Fig. 3: Our framework of qubit mapping.

A. Initial Placement

The initial placement places the circuit inputs to certain physical qubits and renders a list of gates as the initial Waitlist. We exploit two heuristic approaches, the static and the depth-first search (DFS) placements. The static placement assigns the logical qubits to the physical qubits with the same indices as defined in the quantum circuit. The DFS placement starts by assigning the first logical qubits in the DFS list to an arbitrary physical qubit and then continues placing the input qubits by the DFS list to the neighboring physical qubits on the device. The DFS placement makes each two input qubits required by the gates rather close.

Intuitively speaking, the DFS placement should generate a better result for the qubit mapping problem. However, in our observations, its advantage over the static placement is quite minor. This may be due to the vast search space of the problem and thus the effect of the initial placement attenuates quickly during the mapping process. Nevertheless, we use DFS placement as the default in our framework.

B. Routing: Duostra (Dual-source Dijkstra)

Given a two-qubit gate that operates on two physically remote qubits, the routing algorithm explores the possible routing paths and outputs a route of SWAP sequence that brings the two operating bits to an adjacency. In this paper, we introduce a novel routing algorithm, Duostra (Dual-source Dijkstra), in which the finishing time of the SWAP sequence is optimized given a gate on the dependency graph. We also show that the time complexity of this algorithm is $O(nlgn)$, where n is the number of qubits of the device.

In the following, we first introduce two important terminologies, “occupied time” and “routing path”, for our routing algorithm and then present the details of the algorithm in the end.

1) *Occupied Time*: We adopt the concept as introduced in [13] to define the “occupied time” of a qubit. When a physical qubit is involved in an operation (e.g. SWAP, CX, etc), it is occupied by the operation. If an operation is executed from τ_0 to τ_1 on a physical qubit Q_n , we define the occupied time

of Q_n as the finishing time of the operation and denote it as $Q_n.ocp = \tau_1$, which means that the qubit cannot be assigned to another operation until τ_1 .

We can further extend the concept of occupied time to the edge on the Device Graph. Let $e(i, j)$ be an edge that connects two adjacent qubits Q_i and Q_j on $DevG$. Applying a SWAP gate on this edge will swap the logical qubits that Q_i and Q_j carry. We can then calculate the occupied time for the edge with or without applying SWAP by:

$$e(i, j)_{swap.ocp} \triangleq \max(Q_i.ocp, Q_j.ocp) + \tau_{swap} \text{ with SWAP} \quad (1)$$

$$e(i, j).ocp \triangleq \max(Q_i.ocp, Q_j.ocp) \text{ without SWAP} \quad (2)$$

where $Q_i.ocp$, $Q_j.ocp$ and τ_{swap} represent the occupied time of Q_i , occupied time of Q_j , and the operating time for a SWAP gate (i.e. 6 units as defined in [13] and [14]).

2) *Routing Path*: Given a source qubit Q_s and a remote target qubit Q_t , we denote the routing path $RP(s, t)$ as a path from Q_s to Q_t where a sequence of SWAPs is applied along the edges on the path.

Let Q_1, Q_2, \dots, Q_n be the n qubits between Q_s and Q_t along the routing path $RP(s, t)$. In other words, Q_s and Q_1 , Q_i and Q_{i+1} (for i between 1 and $n-1$), and Q_n and Q_t are all adjacent. With Eq. (1), we can recursively calculate the occupied time of a routing path as

$$\begin{aligned} RP(s, t).ocp &= \max(RP(s, n), e(n, t)_{swap.ocp}) \\ &= \max(\max(RP(s, n-1), e(n-1, n)_{swap.ocp}), \\ &\quad e(n, t)_{swap.ocp}) = \dots, \end{aligned}$$

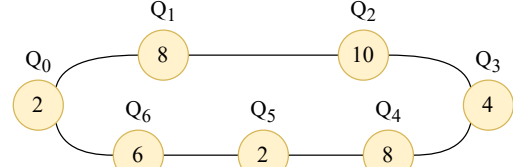
where $e(n-1, n)$ and $e(n, t)$ are adjacent edges between Q_{n-1} and Q_n , and Q_n and Q_t , respectively.

Note that when we compute the occupied time of a routing path, the occupied time of the qubits along the path will be updated as well. Taking Fig. 4 as an example, let Q_0 and Q_3 be the two physical qubits to swap and the occupied time of each qubit is denoted in the nodes of the graph (Fig. 4(a)). If we choose Q_0 as the source and Q_3 as the target, we can see that the SWAPs can be operated along two paths (Q_0, Q_1, Q_2, Q_3) or $(Q_0, Q_6, Q_5, Q_4, Q_3)$. The occupied time for these two routing paths and the corresponding qubits is calculated as shown in Fig. 4(b). Since the occupied time of the path (Q_0, Q_1, Q_2, Q_3) (i.e. 26) is smaller than that of the path $(Q_0, Q_6, Q_5, Q_4, Q_3)$ (i.e. 30), we can ignore the latter for future consideration in optimizing the execution time of the quantum circuit. In general, given a source qubit Q_s and a target qubit Q_t , we denote their optimal routing path as $RP_{opt}(s, t)$. In this example, $RP_{opt}(0, 3) = 26$.

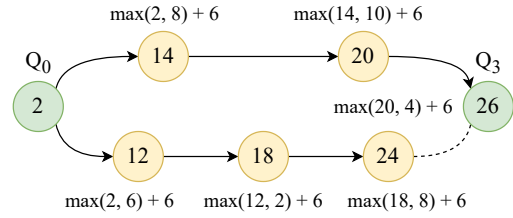
It is also worthwhile to note that if we switch the roles of the source and target qubits for Q_0 and Q_3 , the occupied time for the routing path and the qubits will be different. Fig. 4(c) details the calculation of the occupied time for the routing paths and qubits when taking Q_3 as the source and Q_0 as the target. We can see that $RP_{opt}(3, 0)$ is equal to 28, which is

larger than $RP_{opt}(0, 3)$ (i.e. 26). Therefore, making Q_0 as the source and Q_3 as the target will be a better routing path.

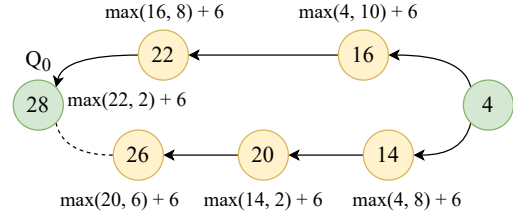
However, if we treat both Q_0 and Q_3 as sources and try to find two routing paths to meet in the middle, as shown in Fig. 4(d), we can further improve the occupied time. This leads us to the Duostra routing algorithm.



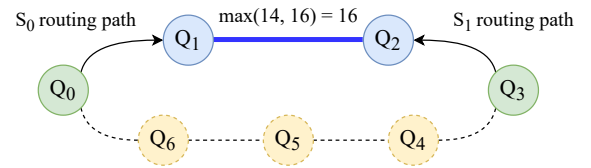
(a) Occupied time of the qubits



(b) Occupied time of the routing path $RP(0,3)$



(c) Occupied time of the routing path $RP(3, 0)$



(d) Duostra search for the optimal routing path: $RP(0,1) + RP(3,2)$

Fig. 4: Demonstration of the Duostra Procedure

3) *The Duostra Algorithm*: Take Fig. 4 as an example again. If we treat both Q_0 and Q_3 as sources, and try to search for two routing paths between them, we can see that when both routing paths meet at the edge $e(1, 2)$, we can obtain an optimal routing path with the minimal occupied time 16. In other words, by swapping the logical qubits on Q_0 to Q_1 and on Q_3 to Q_2 , we can bring the computation of the two-qubit gate to a pair of adjacent qubits and achieve the optimal qubit mapping for it.

The dual-source routing algorithm, called ‘‘Duostra’’, is depicted as the following:

Given a two-qubit gate that operates on two physically remote qubits (i.e. the sources) Q_{s_0} and Q_{s_1} , Duostra algorithm

finds a pair of adjacent qubits (i.e. the targets) Q_{t_0} and Q_{t_1} on the Device Graph such that the maximum of $RP_{opt}(s_0, t_0).ocp$ and $RP_{opt}(s_1, t_1).ocp$, can be minimized. That is:

$$\min_{e \in E} (\max(RP_{opt}(s_0, t_0).ocp, RP_{opt}(s_1, t_1).ocp)) \quad (3)$$

The Duostra algorithm can be implemented similarly to the classic shortest-path finding algorithm, the Dijkstra's algorithm [16], except that our search tree is starting from dual sources. We present the pseudo code of the Duostra algorithm in Algorithm 1 below.

Algorithm 1 Dual-source Dijkstra (Duostra)

```

1: procedure DUOSTRA( $Graph, s_0, s_1$ )
2:    $s_0.source \leftarrow s_0$ 
3:    $s_1.source \leftarrow s_1$ 
4:    $PQ \leftarrow$  priority queue
5:   pushUnseenNeighbors( $PQ, s_0$ )
6:   pushUnseenNeighbors( $PQ, s_1$ )
7:   while  $PQ$  is not empty do
8:      $m \leftarrow$  nodeWithLowestCost( $PQ$ )
9:     Visit( $m$ ) ▷ Mark  $m$  as visited
10:    if  $\exists$  visited neighbor  $v$  s.t.  $m.source \neq v.source$ 
11:      then
12:         $RP(m.source, m) \leftarrow$  backtrace( $m$ )
13:         $RP(v.source, v) \leftarrow$  backtrace( $v$ )
14:        return ( $path_{s_0}, path_{s_1}$ )
15:      end if
16:      pushUnseenNeighbors( $PQ, m$ )
17:    end while
18:  end procedure
19: procedure PUSHUNSEENNEIGHBORS( $PQ, m$ )
20:   for  $v \in$  Neighbor( $m$ ) and  $v.unseen$  do
21:      $v.source \leftarrow m.source$ 
22:      $v.seen \leftarrow True$ 
23:      $PQ.push(v)$ 
24:   end for
25: end procedure

```

First, we initialize a priority queue, PQ , and mark all vertices $v \in V$ as unseen and unvisited. The input sources of the routing problem, s_0 and s_1 , are then marked as seen and visited. For each vertex v , we use a field $v.source$ to denote its routing source. Clearly, there are only two possible routing sources s_0 and s_1 , and we set the routing sources of s_0 and s_1 as themselves (Lines 2 and 3). Then we push all the adjacent vertices of s_0 and s_1 to PQ with the updated occupied time, mark them as seen, and record their sources as either s_0 or s_1 (Lines 5 and 6). Next, we iteratively take the vertex with the smallest occupied time, m , out from PQ and mark it as visited (Lines 8 and 9). If there exists an adjacent vertex v of m that is visited and is routed from the other source different from $m.source$ (Line 10, i.e. $v.source \neq m.source$), then we can conclude the procedure and constitute an optimal routing solution by the optimal routing path from $m.source$ to m (i.e. $RP_{opt}(m.source, m)$), the optimal routing path from

$v.source$ to v (i.e. $RP_{opt}(v.source, v)$), and the edge $e(m, v)$ (see Section IV for the proof of the optimality of the Duostra algorithm). Otherwise, we push all the unseen neighbors of m to PQ and continue.

Note that we need not record the search trees from the dual sources s_0 and s_1 in different priority queues. Instead, we record all the seen vertices in a single priority queue, no matter if their sources are s_0 or s_1 . As we define the cost of a seen vertex v in the priority queue as the occupied time of the optimal routing path from $v.source$ to v , the top vertex in the priority queue, which has the lowest cost, will be the earliest qubit that can be applied with a swap gate.

Besides, the cost of a vertex does not change once the vertex is pushed into the priority queue. Thus, we can guarantee that when two search trees from s_0 and s_1 meet each other at a pair of adjacent physical qubits, it must form the optimal routing path with the smallest occupied time. This is because if there exists another sequence that can be finished earlier, it must have been visited from the priority queue and terminated the search process earlier. See Section IV-A for the proof on the optimality of the priority queue.

C. Scheduling

Given a quantum circuit, the scheduler determines an execution sequence of the gates in order to optimize the total execution time (or some other objectives) on the quantum computing device. Please note that at any moment, we can select any gate from the Waitlist for the next execution and evoke the Duostra algorithm to find an optimal routing path for the SWAP insertions. After a gate is executed and SWAPs are performed, the occupied time of the related qubits are updated and the subsequent gates on the Dependency Graph are added to the Waitlist. Since different execution orders can lead to different execution time, in order to obtain the global optimum of the scheduling problem, we need to enumerate all the execution sequences of the gates (i.e. different gate selections from the Waitlist). This turns out to be an intractable task even for a small scale of quantum circuit. Therefore, in this paper, we propose two heuristic approaches that exploit different subsets of the execution sequences at each step for picking the gate to route in the next execution.

1) *Limitedly-Exhaustive (LE) Search*: Since enumerating all possible gate sequences on the Dependency Graph is exponentially expensive, we devise a Limitedly-Exhaustive Search to limit the search depth of each decision. That is, given a depth limit of d as specified by the user, all the depth- d sequences from any gate in the Waitlist are exhaustively searched and their corresponding occupied time is calculated by the Duostra routing algorithm. The scheduler then selects the sequence with the minimal occupied time, picks up its corresponding gate in the Waitlist to execute, updates the Waitlist, and then repeats the process for the subsequent depth- d sequences. For example, if the depth equals 2, the LE Search will first enumerate all the gates in the Waitlist, find the optimal routing path of each gate by Duostra, and update the corresponding occupied time and Waitlists. Subsequently, for

each gate in the previous iteration and its updated Waitlist, we enumerate the gates in the updated Waitlist and repeat the above process again. Finally, the gate that leads to the smallest occupied time in these depth-2 sequences will be picked for the execution, and the above LE search will be restarted.

2) *Shortest-Path (SP) Estimation*: Although the LE Search heuristic may closely approximate the global optimum solution given a large enough search depth d , however, due to the massive calculations from the path enumeration, it can only be applicable for small designs. Therefore, inspired by Li *et al.* [12], we propose another heuristic by considering the shortest path [17] between the physical qubits of the gate. Let g_i be a gate in the Waitlist, $g_i.Q_i$ and $g_i.Q_j$ be the current qubit assignments of this two-qubit gate, and $SP(g_i.Q_i, g_i.Q_j)$ be the shortest path between the qubits. Then the SP-Estimation goes through all the gates in the Waitlist and selects the one with the minimal value of this equation:

$$\max(g_i.Q_i.ocp, g_i.Q_j.ocp) + c \cdot SP(g_i.Q_i, g_i.Q_j), \quad (4)$$

where c is a constant factor to estimate the execution time of the shortest path. Once a gate from the Waitlist is selected, we apply the Duostra algorithm to compute the occupied time of the circuit, and repeat.

The time complexities of the SP Estimation and LE Search are $O(N(W + R))$ and $O(N^2n)$, respectively, where N and W are the number of gates in the circuits and the Waitlist, R is the time complexity of the router, and n is the number of qubits.

To sum up, the LE Search approach exploits all the possible gate sequences for a given depth d . It can acquire the global optimum solutions for smaller designs as the depth d can be made large enough. On the other hand, the SP Estimation trades some performance for better scalability and thus can be applied to large circuits towards quantum advantage.

IV. PROOF OF DUOSTRA OPTIMALITY

A. The optimality of priority queue

The physical qubits are modeled as the vertices. During the Duostra search, the vertices (v) would be classified into three types, visited (ν), seen (ξ), and unseen vertices (μ), respectively. In the beginning, the sources would be labeled visited, and the adjacent vertices of the sources would be labeled seen. In each iteration, the algorithm would select a vertex within the set of seen vertices. Subsequently, the unseen vertices which are connected to the selected visited vertex would be labeled seen.

Each vertex v_i has a cost C based on its parent v_{p_i} .

$$C(v_{p_i}, v_i) = \max(v_{p_i}.ocp, v_i.ocp) + \tau_{swap} \quad (5)$$

indicates the cost of searching path from v_{p_i} to v_i . In Duostra algorithm, the seen vertices would be added into a priority queue with its cost calculated by Eq. (5). The priority queue would output a vertex with the minimum cost among all the seen vertices. The unseen vertex μ_j must be connected to seen set

$$S_{seen} = \bigcup_{i \in \mathcal{V}} \xi_i$$

by at least one edge. We assume μ_j to be connected to an arbitrary $\xi_0 \in S_{seen}$ in an edge, we have

$$\begin{aligned} C(\xi_0, \mu_j) &= \max(\xi_0.ocp, \mu_j.ocp) + \tau_{swap} \\ &> \xi_i.ocp \geq \min_i(\xi_i.ocp), \end{aligned} \quad (6)$$

By Eq. (6), we can find that the cost of a child must be greater than the cost of the parent of this child. The unseen vertex must be connected to an seen vertex ξ_i by at least an edge, therefore, the unseen vertex will has the cost bigger than ξ_i . Hence, we conclude that the priority queue would output the vertex with the smallest cost among all unvisited vertices.

B. The optimality of Duostra

In the routing problem, we meant to find an edge e^* between two adjacent vertices, v_0^* and v_1^* , to minimize the objective function $\max(RP(s_0, v_0^*), RP(s_1, v_1^*))$ given two sources s_0 and s_1 .

In this scenario, the vertices of the two paths formed by the two sources are pushed into the same priority queue. With the property of priority queue demonstrated in Section IV-A, the vertices of two sides would be popped according to the cost. Therefore, the first edge where the two sides meet first has the smallest cost, which would be e^* .

Suppose Duostra finds a sub-optimal edge e^- with two vertices, v_0^- and v_1^- . The cost of the solution is

$$\max(RP(s_0, v_0^-), RP(s_1, v_1^-)).$$

Since

$$\begin{aligned} \max(RP(s_0, v_0^-), RP(s_1, v_1^-)) &> \\ \max(RP(s_0, v_0^*), RP(s_1, v_1^*)), \end{aligned} \quad (7)$$

the two paths in the optimal solution must be found before the path with higher cost in the suboptimal solution due to the optimality of the priority queue. This means that Duostra can always find the optimal solution to the qubit mapping routing problem.

V. EXPERIMENTAL RESULTS

In this section, we present the superiority of our framework in three aspects: scalability, performance, and flexibility.

First, for scalability, our algorithm is able to tackle the 11,969-qubit Quantum Fourier Transform (QFT) circuit and finishes the qubit mapping within 5 hours. Besides, experimental results show that the growth of the execution time of the quantum circuits as well as the program runtime of our algorithm are both less than $O(n^3 \lg n)$, indicating that our algorithm is very scalable as the qubit number (n) increases so as to achieve quantum advantage.

Second, on top of the fact that our program can run much faster than the state-of-the-art mapping schemes, it also produces better qubit mapping results in terms of the execution time of the quantum circuits. In particular, our SP Estimation method proposes up to 33% improvement over the IBM Qiskit Mapping [18] on the 127-qubit QFT. On the other hand, our LE Search method has a 5% improvement on average when

TABLE I: Experimental results on the scalability of our framework.

#Q	Ideal	TOQM	LE Search		SP Estimation	
		Cost	Cost	Ratio	Cost	Ratio
11,969*	83,779	TLE	TLE	∞	3,049,728	36.40
7,073*	49,507	TLE	TLE	∞	1,428,287	28.85
5,105*	35,731	TLE	TLE	∞	808,289	22.62
3,457*	24,195	TLE	TLE	∞	539,573	22.30
2,129*	14,899	TLE	TLE	∞	322,788	21.67
1,121*	7,843	TLE	TLE	∞	163,956	20.90
433	3,027	TLE	TLE	∞	57,378	18.96
127	885	TLE	14,734	16.65	13,902	15.70
65	451	TLE	4,890	10.84	5,520	12.24
27	185	1,155	1,116	6.03	1,552	8.39
16	108	438	480	4.44	650	6.02
7	45	128	125	2.77	146	3.24
5	31	71	62	2.00	76	2.45

compared to the Time Optimal Qubit Mapping (TOQM) [14] on the small quantum circuit benchmarks provided by SABRE.

Finally, as for flexibility, we conducted experiments on some large oracle circuits taken from the classical Electronic Design Automation (EDA) benchmarks ISCAS-85 [19]. The results show that our algorithm had advantages not only for specific QFT circuits but also for the general oracle circuits. In addition, by parameterizing different scheduling heuristics, our algorithm can also be flexible in trading off between optimality and flexibility for different types and sizes of quantum circuits.

We conducted the experiments on Intel® Xeon® CPU E5-2630 v4 @ 2.20GHz with total 126G memory.

A. Scalability

We tested the scalability of our proposed mapping algorithm by QFT circuits of different sizes. We chose QFT because it can be easily scaled up and is regarded as one of the most difficult test sets since each of its qubits has to interact with all the other qubits. The QFT circuits were generated following the method proposed in [1]. However, due to the limitation of the basic gate set on IBMQ machines, we decomposed all CR and H gates in the circuit. As for the Devices Graph of the quantum computers more than 433 qubits and beyond, we followed the topological patterns of the existing IBM machines and extrapolated them up to 11,969 qubits in order to test the algorithm scalability.

The experimental results are presented in Table I, in which we compared the scalability of three different methods: state-of-the-art TOQM⁴ [14], our LE search, and our SP estimation method. The time limit for the program runtime was 5 hours; thus the results labeled TLE represent “time limit exceeded”. The results are the execution time of the mapped circuits (also referred as “cost” in the following), which follow the “cost” definition proposed in CODAR [13] and computation criteria from TOQM [14]. The execution time of the single-qubit gates, double-qubit gates (CX), and SWAP gates were 1,

⁴When running the TOQM program, we followed the default parameters given by the source code for small cases. For cases labeled TLE, we set the depth to 1 (the minimum) but still got “time limit exceeded”.

TABLE II: Performance comparison with IBM Qiskit [18] on QFT circuits.

#Q	Only Mapping			With Synthesis		
	#Gate	SP Est.	Qiskit	#Gate	SP Est.	Qiskit
127	32,385	13,902	20,888	8,279	8,124	8,940
65	8,515	5,520	7,440	3,939	3,982	4,300
27	1,485	1,552	2,065	1,279	1,543	1,838
16	528	650	578	513	737	970
7	105	146	137	99	173	205
5	55	76	69	44	90	107

2, and 6, respectively. “Ideal” in the second column represents the mapping cost on a fully-connected ideal device, indicating that quantum gates can be mapped to arbitrary qubits and no SWAP will be needed. “Ratio” is defined as $C_{Proposed}/C_{Ideal}$, which is the ratio in terms of the cost of the proposed method on the IBM machine over the ideal device.

As indicated in Table I, TOQM can only work on QFTs up to 27 qubits, which is far from the goal of achieving quantum advantage. Compared to TOQM, our LE Search method demonstrates the improvements on both optimization results and scalability. On the other hand, our SP Estimation heuristic, although sacrificing a little bit on the optimization results, is the only method that can be scaled up to handle QFTs of thousand qubits and beyond. However, it is interesting to see that SP Estimation actually outperforms LE Search method on the 127-qubit QFT case. This is mainly due to the fact that LE search is barely able to handle circuits of this size and thus the result is farther from the optimum. This also indicates that the quality of the optimization results by SP Estimation is pretty good, considering that there is no way to estimate what the global optimum is.

To sum up, by applying the Duostra in Algorithm 1 and the scheduler guided by the SP estimation, the cost (i.e. the circuit execution time) complexity will be $O(n^3)$ since each gate requires $O(n)$ for execution in the worst case and the number of gates in QFT is $O(n^2)$. However, the experiment results show that the cost is in the order of $n^{1.3}$ with respect to the number of qubits. For the program runtime, theoretically the time complexity is $O(N(n \lg n + W))$, where N and W are the number of gates in the circuits and the Waitlist, respectively. Therefore, we have the time complexity $O(n^2(n \lg n + n)) = O(n^3 \lg n)$ for QFT circuits since QFT can only have at most $O(n)$ gates in the Waitlist simultaneously. By taking logarithm on numbers of qubits and runtime from the experimental results, the empirical complexity here is $O(n^{2.8})$. The polynomial complexity ensures the scalability of our algorithm and the capability to achieve the quantum advantage.

B. Performance

To evaluate the performance of our mapping algorithm, we compared the qubit mapping cost of our method with the state-of-the-art results in two test sets, the QFTs up to 127 qubits⁵

⁵Although Osprey (433) has been released, Qiskit does not support it currently.

TABLE III: Performance comparison with TOQM on quantum benchmark circuits

Benchmark	#Q	#Gate	Ideal	TOQM [14]		SP Estimation				LE Search			
				Cost	Time	Cost	Time	$\Delta(\%)$	T	Cost	Time	$\Delta(\%)$	T
cm82a_208	8	650	571	1,554	2.25	1,688	0.32	-8.62	7.0	1,495	0.53	3.80	4.3
rd53_251	8	1,291	1,203	3,348	4.20	3,515	0.31	-4.99	13.5	3,192	0.45	4.66	9.4
urf2_277	8	20,112	19,698	59,989	75.53	60,464	0.32	-0.79	239.0	55,126	3.07	8.11	24.6
urf1_278	9	54,766	53,256	160,414	199.74	160,964	0.41	-0.34	484.8	147,591	8.33	7.99	24.0
hwb8_113	9	69,380	64,758	183,657	224.49	192,203	0.41	-4.65	544.9	172,575	10.77	6.03	20.8
urf1_149	9	184,864	172,518	466,086	559.38	479,559	0.60	-2.89	937.0	437,037	39.48	6.23	14.2
rd73_252	10	5,321	4,829	13,869	16.37	14,377	0.31	-3.66	53.0	12,895	1.53	7.02	10.7
sqn_258	10	10,223	9,176	26,502	33.58	27,469	0.32	-3.65	104.0	24,496	3.48	7.57	9.6
z4_268	11	3,073	2,756	7,887	10.98	8,323	0.31	-5.53	35.4	7,441	1.24	5.65	8.9
life_238	11	22,445	20,867	58,932	69.75	63,330	0.34	-7.46	204.6	56,546	4.67	4.05	14.9
9symml	11	34,881	32,084	90,976	111.17	97,089	0.43	-6.72	257.3	86,615	7.14	4.79	15.6
sqrt8_260	12	3,009	2,779	7,863	9.92	8,462	0.30	-7.62	32.7	7,561	1.57	3.84	6.3
cycle10_2	12	6,050	5,662	15,988	20.00	17,008	0.29	-6.38	69.4	15,321	1.87	4.17	10.7
rd84_253	12	13,658	12,176	34,876	43.57	37,120	0.31	-6.43	139.2	33,019	3.71	5.32	11.7
adr4_197	13	3,439	3,088	8,859	10.92	9,186	0.32	-3.69	34.2	8,225	2.55	7.16	4.3
root_255	13	17,159	14,799	42,969	54.88	45,645	0.33	-6.23	166.8	40,671	12.35	5.35	4.4
dist_223	13	38,046	32,968	95,648	123.30	101,841	0.36	-6.47	340.6	90,288	12.38	5.60	10.0
cm42a_207	14	1,776	1,574	4,472	5.84	4,587	0.30	-2.57	19.4	4,245	3.77	5.08	1.5
pm1_249	14	1,776	1,574	4,472	5.79	4,587	0.33	-2.57	17.6	4,245	5.25	5.08	1.1
cm85a_209	14	11,414	10,630	30,157	37.18	32,298	0.35	-7.10	105.3	29,076	2.82	3.58	13.2
sqrt_7	15	7,630	6,367	18,049	25.84	19,296	0.31	-6.91	82.8	17,621	2.20	2.37	11.7
ham15_107	15	8,763	8,092	23,048	31.60	24,395	0.35	-5.84	91.3	21,652	3.97	6.06	8.0
dc2_222	15	9,462	8,759	24,872	31.40	26,532	0.31	-6.67	101.9	23,773	4.66	4.42	6.7
inc_237	16	10,619	9,790	27,256	34.45	29,651	0.34	-8.79	102.5	26,500	5.87	2.77	5.9
mlp4_245	16	18,852	17,258	48,990	62.52	52,839	0.36	-7.86	171.7	47,199	6.95	3.66	9.0

(larger sizes) and the quantum circuit benchmarks introduced by SABRE (smaller sizes) [12].

1) *QFT*: As shown in Table I, since the state-of-the-art method TOQM can only handle QFT circuits up to 27 qubits, we conducted the experiments for performance comparison with IBM Qiskit [18] [20] only. The results are presented in Table II. We conducted two sets of experiments: “Only Mapping” means we tested directly on the circuits as described in Section V-A, and “With Synthesis” implies that we applied the Qiskit synthesis tool on circuits from “Only Mapping”. The results are compared with our SP Estimation heuristic. Note that circuit synthesis followed by qubit mapping are two recommended steps in the Qiskit transpiler flow. For Qiskit Synthesis, we set the optimized level to 2, and for Qiskit Mapping we set the optimized level to 0.

The experimental results in Table II demonstrate that our method can outperform IBM Qiskit on both “Only Mapping” and “With Synthesis” tests for 33.4% and 8.3% in terms of the costs (i.e. circuit execution time) of the mapped circuits. Our advantages actually manifest as the number of qubits increases. This again signifies our advancements in pursuing the quantum advantage.

2) *Quantum Circuit Benchmark*: We conducted the second set of experiments for performance evaluation for the quantum benchmark circuits proposed in SABRE [12]. The circuits are a subset of RevLib [21] and are decomposed into single- and two-qubit gates. They are up to 16 qubits and in varied sizes of 650 to 185,000 gates. We took the results of TOQM [14] as the baseline, as it claimed the mapping optimality by exhaustive search on the benchmarks. The results are compared with both of our LE Search and SP Estimation heuristics.

Besides, for fair comparison, we ran all the experiments on *ibmq_guqdalupe*, which is a 16-qubit machine ⁶.

The experimental results are listed in Table III. In this table, we list both optimization results and program runtime for SP Estimation, LE Search (with depth set to 4), and the baseline from TOQM [14]. For the SP Estimation heuristic, although the optimization results are slightly inferior to the baseline (mostly 6 – 9%), our program runs significantly faster ($7\times$ to $937\times$) than TOQM. As for LE Search, we outperformed TOQM on both optimization results ($\approx 5\%$ on average) and speed ($\approx 10\times$ on average). The results indicate that although we sacrifice some degree of optimality by applying heuristic approaches in scheduling the gate sequences, the efficient and optimality-ensured Duostra router can serve as a powerful engine in optimizing the mapping solutions for the quantum gates. We need not settle for the exhaustive yet non-scalable approaches as in TOQM. Overall, our integrated framework provides a practical qubit mapping solution for the future quantum advantage.

C. Flexibility

To achieve global optimality of the qubit mapping problem, we need to at least enumerate all the gate sequences from the Waitlist in finding the optimal routing paths of the two-qubit gates. This is definitely intractable for any reasonable size of circuits and the experimental results of the exhaustive-search-based approach TOQM has indicated this limitation (i.e. only

⁶In the original Time Optimal Qubit Mapping (TOQM) paper, the experiments were conducted on an IBM Tokyo machine. However, this device is no longer provided by IBMQ. Hence, we changed the device to *ibmq_guadalupe* and re-ran the experiments with the source code.

TABLE IV: Results of the oracles transformed from classical EDA circuits to XMG by ABC tool [22].

Benchmark	#Q	#Gate	Ideal	SP Estimation			LE Search				
				Cost	Ratio	Time	Cost	Ratio	Time	$\Delta(\%)$	T
q499_xmg	172	2,586	1,576	4,630	2.94	0.90	4,462	2.83	1.14	3.63	0.79
q1355_xmg	188	2,558	1,167	3,705	3.17	0.91	3,453	2.96	1.10	6.80	0.83
q432_xmg	202	4,137	967	3,612	3.74	0.86	3,214	3.32	2.01	11.02	0.42
q1908_xmg	255	5,184	1,382	4,850	3.51	0.93	4,809	3.48	1.36	0.85	0.68
q2670_xmg	660	12,720	1,298	6,199	4.78	4.79	5,795	4.46	33.43	6.52	0.14
q6288_xmg	840	30,653	2,958	13,545	4.58	4.91	12,502	4.23	67.74	7.70	0.07
q3540_xmg	991	25,784	3,455	14,154	4.10	4.94	13,849	4.01	41.38	2.15	0.12
q7552_xmg	1,380	27,453	4,839	15,006	3.10	40.83	14,741	3.05	171.80	1.77	0.24
q5315_xmg	1,573	33,588	1,921	12,297	6.40	40.28	11,231	5.85	401.26	8.67	0.10

up to 27-qubit QFT). Therefore, to serve as a practical qubit mapping tool, it is essential to provide flexibility in dealing with different types and sizes of the quantum circuits.

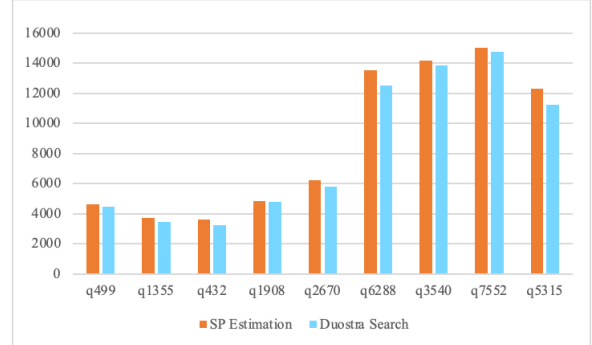
We have demonstrated the scalability of our approach by QFT circuits in Section V-A. Here we tested the flexibility of our tool by conducting experiments on classical EDA circuits [19]. We prepared the quantum circuits as follows. We first transformed the benchmark circuits into XOR-Majority Graph (XMG) by the ABC tool [22], which has a direct mapping onto the X, CX, and Toffoli gates in a quantum circuit. We finally decomposed the Toffoli gates into single- and two-qubit gates in the quantum cell library. Column 3 “#Gates” in Table IV lists the number of quantum gates of these benchmark circuits.

We conducted the experiments with both the SP Estimation and LE Search heuristics. The columns “Ideal” and “Ratio” have the same definitions as in Table I of Section V-A. As shown in the results, we have ratios ranging from 2.94 to 6.40 for these large-scale oracle benchmarks for SP Estimation and 2.83 to 5.85 for LE Search. Although it is not possible to evaluate how far these numbers are from global optimality, yet for comparison purposes, let’s refer to the results of the 433- and 1121-qubit QFT circuits in Table I, which are of the similar size and number of qubits. The performance ratios of these two QFT circuits are around 20, which is much larger than the EDA benchmark circuits. Therefore, we can safely conclude that our qubit mapping algorithm works reasonably well on these benchmark circuits.

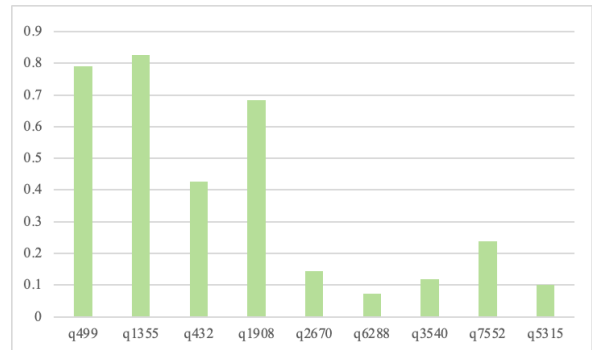
To further testify the flexibility of our framework, we compared the optimization results and runtime for LE Search and SP Estimation approaches as shown in Fig. 5. As Fig. 5(a) shows, the LE Search approach, which applies exhaustive search with a limited depth, can consistently generate better optimization results on circuit execution time. However, the SP Estimation heuristic can run faster than LE Search, especially when the design sizes get bigger. In conclusion, our framework has the flexibility to deal with different types and different sizes of quantum circuits.

VI. CONCLUSION

In this paper, we propose a novel framework to tackle the qubit mapping problem for large-scale quantum algorithms aiming for quantum advantage. Our framework is composed of three major components – placement, routing, and scheduling.



(a) Comparison of optimization results



(b) Runtime comparison (SP Estimation / LE Search)

Fig. 5: Comparison of LE Search and SP Estimation on ISCAS85 benchmark circuits

The initial placement step can quickly place the circuit inputs to certain physical qubits, and the Duostra routing algorithm can efficiently identify the optimal swapping path for the two-qubit gates. The scheduler is to determine the gate sequence for the mapping process. With the SP Estimation and LE Search heuristics, the scheduler can provide the flexibility in striking the balance between runtime and optimization quality. We have conducted experiments on various sets of benchmarks and the experimental results demonstrate our superiority in scalability, performance, and flexibility. To the best of our knowledge, we are the first to solve the qubit mapping problem for circuits up to 11,969 qubits, which have successfully demonstrated the capability of achieving quantum advantage.

REFERENCES

- [1] M. A. Nielsen and I. L. Chuang, *Quantum Computation and Quantum Information: 10th Anniversary Edition*, 2010.
- [2] “40 years of quantum computing,” *Nature Reviews Physics*, vol. 4, no. 1, pp. 1–1, Jan. 2022.
- [3] S. Khatri and M. M. Wilde, “Principles of quantum communication theory: A modern approach,” *arXiv:2011.04672*, 2020.
- [4] C.-Y. Chen, G.-J. Zeng, F. jhu Lin, Y.-H. Chou, and H.-C. Chao, “Quantum cryptography and its applications over the internet,” *IEEE Network*, vol. 29, no. 5, pp. 64–69, Sep. 2015.
- [5] S. Arunachalam and R. de Wolf, “A survey of quantum learning theory,” 2017.
- [6] IBM Newsroom, “IBM unveils 400 qubit-plus quantum processor and next-generation IBM quantum system two,” Nov. 9 2022.
- [7] P. Shor, “Algorithms for quantum computation: discrete logarithms and factoring,” in *Proc. Annual Symposium on Foundations of Computer Science*, 1994, pp. 124–134.
- [8] P. W. Shor, “Polynomial-time algorithms for prime factorization and discrete logarithms on a quantum computer,” *SIAM Journal on Computing*, vol. 26, no. 5, pp. 1484–1509, 1997. [Online]. Available: <https://doi.org/10.1137/S0097539795293172>
- [9] J. Proos and C. Zalka, “Shor’s discrete logarithm quantum algorithm for elliptic curves,” *arXiv preprint quant-ph/0301141*, 2003.
- [10] R. Iten, R. Colbeck, I. Kukuljan, J. Home, and M. Christandl, “Quantum circuits for isometries,” *Phys. Rev. A*, vol. 93, no. 3, p. 032318, 2016.
- [11] M. Y. Siraichi, V. F. d. Santos, C. Collange, and F. M. Q. Pereira, “Qubit allocation,” in *Proc. International Symposium on Code Generation and Optimization*, 2018, pp. 113–125.
- [12] G. Li, Y. Ding, and Y. Xie, “Tackling the qubit mapping problem for nisq-era quantum devices,” in *Proc. International Conference on Architectural Support for Programming Languages and Operating Systems*, 2019, p. 1001–1014.
- [13] H. Deng, Y. Zhang, and Q. Li, “Codar: A contextual duration-aware qubit mapping for various nisq devices,” in *Proc. ACM/IEEE Design Automation Conference (DAC)*, 2020, pp. 1–6.
- [14] C. Zhang, A. B. Hayes, L. Qiu, Y. Jin, Y. Chen, and E. Z. Zhang, “Time-optimal qubit mapping,” in *Proc. ACM International Conference on Architectural Support for Programming Languages and Operating Systems*, 2021, pp. 360–374.
- [15] IBM, “Ibm quantum,” 2021. [Online]. Available: <https://quantum-computing.ibm.com/>
- [16] E. W. Dijkstra, “A note on two problems in connexion with graphs,” *Numerische Mathematik*, vol. 1, no. 1, pp. 269–271, Dec. 1959. [Online]. Available: <https://doi.org/10.1007/bf01386390>
- [17] R. W. Floyd, “Algorithm 97: shortest path,” *Communications of the ACM*, vol. 5, no. 6, p. 345, 1962.
- [18] G. Aleksandrowicz, T. Alexander, P. Barkoutsos, L. Bello, Y. Ben-Haim, D. Bucher, F. J. Cabrera-Hernández, J. Carballo-Franquis, A. Chen, C.-F. Chen *et al.*, “Qiskit: An open-source framework for quantum computing,” *Accessed on: Mar*, vol. 16, 2019.
- [19] F. Brglez, “A neutral netlist of 10 combinational benchmark circuits and a target translator in fortran,” in *Proc. Intl. Symp. Circuits and Systems*, 1985, 1985.
- [20] M. Bozzo-Rey and R. Loredo, “Introduction to the ibm q experience and quantum computing,” in *Proceedings of the 28th Annual International Conference on Computer Science and Software Engineering*, 2018, pp. 410–412.
- [21] R. Wille, D. Große, L. Teuber, G. W. Dueck, and R. Drechsler, “Replib: An online resource for reversible functions and reversible circuits,” in *38th International Symposium on Multiple Valued Logic (ismvl 2008)*. IEEE, 2008, pp. 220–225.
- [22] V. GROUP *et al.*, “Abc: a system for sequential synthesis and verification, release 70930,” 2007.